

Responses of Neurons in the Nucleus of the Basal Optic Root to Translational and Rotational Flowfields

DOUGLAS R. W. WYLIE¹ AND BARRIE J. FROST²

¹Department of Psychology, University of Alberta, Edmonton, Alberta, T6G 2E9; and ²Department of Psychology, Queen's University, Kingston, Ontario K7L 3N6, Canada

Wylie, Douglas R. W. and Barrie J. Frost. Responses of Neurons in the nucleus of the basal optic root to translational and rotational flowfields. *J. Neurophysiol.* 81: 267–276, 1999. The nucleus of the basal optic root (nBOR) receives direct input from the contralateral retina and is the first step in a pathway dedicated to the analysis of optic flowfields resulting from self-motion. Previous studies have shown that most nBOR neurons exhibit direction selectivity in response to large-field stimuli moving in the contralateral hemifield, but a subpopulation of nBOR neurons has binocular receptive fields. In this study, the activity of binocular nBOR neurons was recorded in anesthetized pigeons in response to panoramic translational and rotational optic flow. Translational optic flow was produced by the “translator” projector described in the companion paper, and rotational optic flow was produced by a “planetarium projector” described by Wylie and Frost. The axis of rotation or translation could be positioned to any orientation in three-dimensional space. We recorded from 37 cells, most of which exhibited a strong contralateral dominance. Most of these cells were located in the caudal and dorsal aspects of the nBOR complex and many were localized to the subnucleus nBOR dorsalis. Other units were located outside the boundaries of the nBOR complex in the adjacent area ventralis of Tsai or mesencephalic reticular formation. Six cells responded best to rotational flowfields, whereas 31 responded best to translational flowfields. Of the rotation cells, three preferred rotation about the vertical axis and three preferred horizontal axes. Of the translation cells, 3 responded best to a flowfield simulating downward translation of the bird along a vertical axis, whereas the remaining 28 responded best to flowfields resulting from translation along axes in the horizontal plane. Seventeen of these cells preferred a flowfield resulting from the animal translating backward along an axis oriented $\sim 45^\circ$ to the midline, but the best axes of the remaining eleven cells were distributed throughout the horizontal plane with no definitive clustering. These data are compared with the responses of vestibulocerebellar Purkinje cells.

INTRODUCTION

Because the environment consists of stationary objects and surfaces, as one moves through the environment, optic flow occurs across the entire retina (Gibson 1954). The accessory optic system (AOS) and associated pretectum comprise a distinct visual system dedicated to the analysis of the optic flow that results from self-motion (Frost et al. 1994; Grasse and Cynader 1990; Simpson 1984; Simpson et al. 1988a). In pigeons, this system consists of two major retinal recipient nuclei (Fite et al. 1981; Gamlin and Cohen

1988a; Karten et al. 1977; Reiner et al. 1979): the nucleus of the basal optic root (nBOR) of the AOS and the pretectal nucleus lentiformis mesencephali (LM). Previous studies have shown that most nBOR and LM neurons have large receptive fields and exhibit direction selectivity in response to large-field visual stimuli moving in the contralateral visual field (Burns and Wallman 1981; Gioanni et al. 1984; McKenna and Wallman 1981, 1985; Morgan and Frost 1981; Winterson and Brauth 1985; Wolf-Oberhollenzer and Kirschfeld 1994; Wylie and Frost 1990a, 1996).

The majority of nBOR neurons prefer upward, downward, or backward motion in the contralateral hemifield (Wylie and Frost 1990a), but a small subpopulation of nBOR neurons have binocular receptive fields (Wylie and Frost 1990b). In a previous study, we used two large ($\sim 100 \times 100^\circ$) tangent screen stimuli, one placed on either side of the bird in the central part of each hemifield. Some neurons preferred approximately the same direction of motion in both hemifields, whereas others preferred the opposite direction in both eyes. Such neurons would respond best to flowfields resulting from self-translation and -rotation, respectively. In the present study, we stimulated these binocular neurons with rotational and translational flowfields that occupied the entire visual field. The rotational flowfields were produced by a *planetarium* projector based on that designed by Simpson et al. (1981, 1988b), which we have used to stimulate climbing fiber (CF) activity in the flocculus of pigeons (Wylie and Frost 1993). The translational flowfields were produced by a similar device, which we call a *translator*, which, in the companion paper, we used to stimulate CF activity in the nodulus and ventral uvula in pigeons (Wylie and Frost 1999). A preliminary report of the present study has been published (Wylie et al. 1998a).

METHODS

The methods for anesthesia, surgery, extracellular recording, and data collection are essentially identical to those reported in the companion paper (Wylie and Frost 1999), with a few exceptions outlined in this section. Using the atlas of Karten and Hodos (1967) as a guide, a section of bone and dura was removed from the left side of the skull such that a vertically oriented electrode could access the nBOR. Recordings were made with insulated tungsten microelectrodes having 5- to 10- μm exposed tips.

Translational optic flow stimuli were produced with the *translator* projection described in the companion paper (Wylie and Frost 1999). Rotational flowfields were produced with a *planetarium* projector (Fig. 6A). This consisted of a small, hollow metal cylinder, the surface of which was drilled with numerous small holes.

The costs of publication of this article were defrayed in part by the payment of page charges. The article must therefore be hereby marked “advertisement” in accordance with 18 U.S.C. Section 1734 solely to indicate this fact.

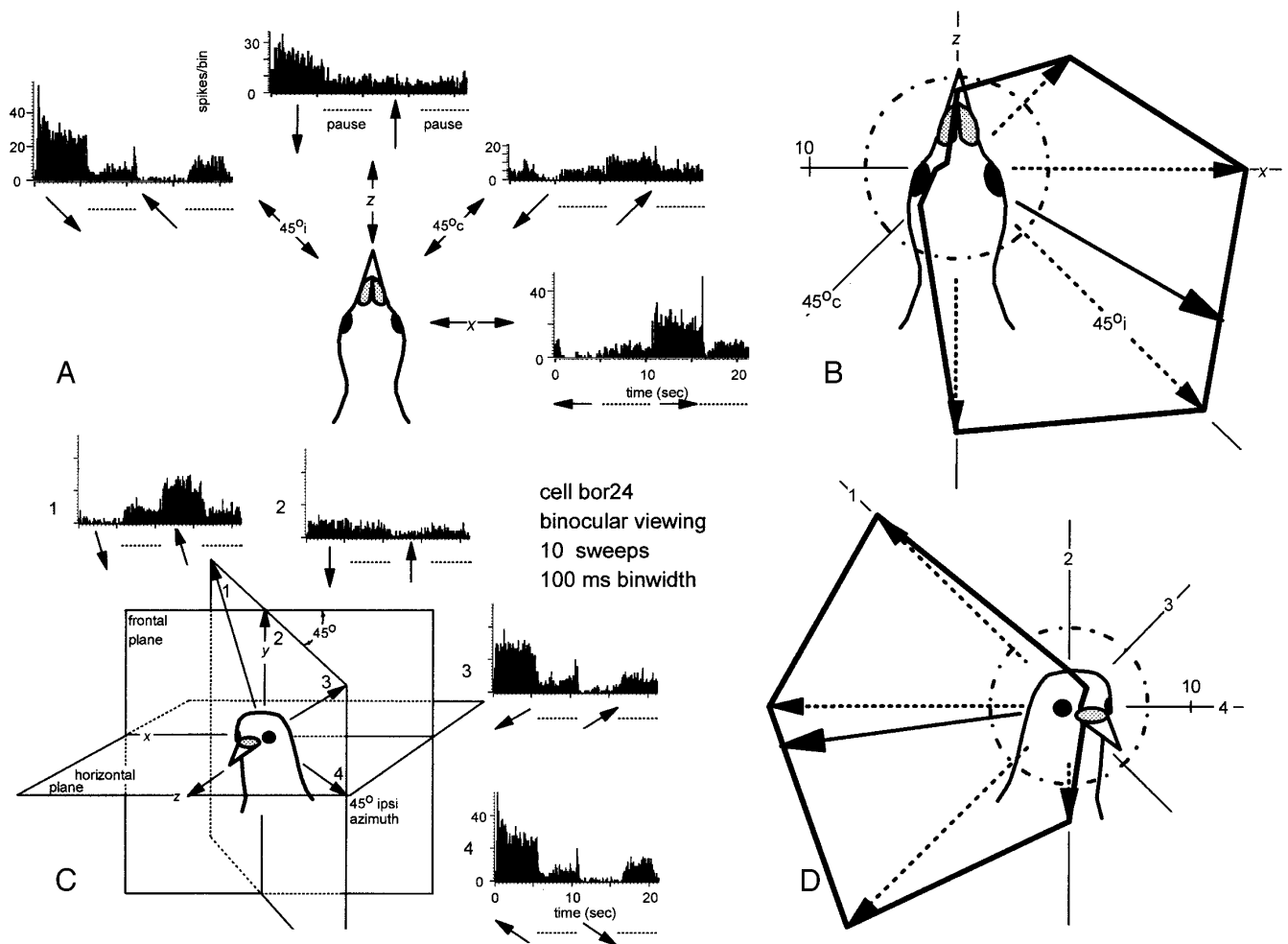


FIG. 1. Responses of a $+x-z$ translation neuron. *A* and *B*: azimuth tuning (in the horizontal plane). *C* and *D*: elevation tuning in a vertical plane that intersects the horizontal plane at 45° ipsilateral (45°_i) azimuth. For clarity, corresponding axes in *C* and *D* are indicated by the numerals 1–4, where axis 2 is the y axis and axis 4 is an horizontal axis at 45°_i azimuth. *A* and *C*: peristimulus time histograms (PSTHs) in response to translational optic flow along 4 axes. Each PSTH is summed from 10 sweeps. For each sweep there was 5.3-s translation in 1 direction, followed by a 5.3-s pause, 5.3-s translation in the opposite direction, and a 5.3-s pause. *B* and *D*: polar plots of the data from *A* and *C*, respectively. Firing rate (spikes/s) is plotted as a function of the orientation of the axis of translational flow in polar coordinates. In *A–D*, the arrowheads point to the focus of expansion (FOE) in the flowfield, i.e., the direction in which the animal would move to cause such a flowfield. *B* and *D*: broken circles, spontaneous firing rate; solid arrows, axis of maximal modulation from the best cosine fit. See text for additional details.

A small filament light source was positioned in its center, and a pen motor, driven by a function generator, oscillated the cylinder about its long axis. We used a frequency of 0.1 Hz, and the dots moved at a constant velocity of $1-2^\circ/s$. The planetarium was suspended above the bird with gimbals such that the axis of rotation could be positioned to any orientation in three-dimensional space.

As with the companion study, once a cell was isolated the direction preference in both hemifields along the interaural axis was determined using a large stimulus ($\sim 90 \times 90^\circ$) consisting of a random pattern of dots and lines. Most cells in the nBOR respond to such stimuli moving in the contralateral visual field. Generally we did not study these monocular cells further. Some cells responded to motion of the hand-held stimulus in both visual fields. These binocular cells showed the same direction preference (translation-sensitive cells) or opposite direction preference in the two hemifields (rotation-sensitive cells). The translation- and rotation-sensitive cells were further studied with a translator and planetarium projector, respectively.

On some penetrations, marking lesions ($30 \mu A$ for 5–10 s) were made at known locations relative to responsive cells. At the end

of the recording session, the animals were killed with an overdose of pentobarbital sodium (100 mg/kg) and perfused transcardially with 0.9% saline followed by 4% paraformaldehyde. The brains were removed and cryoprotected with 20% sucrose, then $40\text{-}\mu\text{m}$ -thick coronal sections were cut with a freezing microtome, and sections through the nBOR were collected, mounted onto gelatin-coated slides, counterstained with neutral red, and a coverslip was applied with Permount.

RESULTS

From 17 pigeons, we recorded the activity of 37 binocular neurons that exhibited direction selectivity in response to large-field moving stimuli. [We also encountered >100 cells with monocular-contralateral receptive fields, but these cells were not further studied as their response properties have been described extensively in previous reports (Morgan and Frost 1981; Wylie and Frost 1990a)]. In response to the hand-held stimulus, 31 neurons preferred

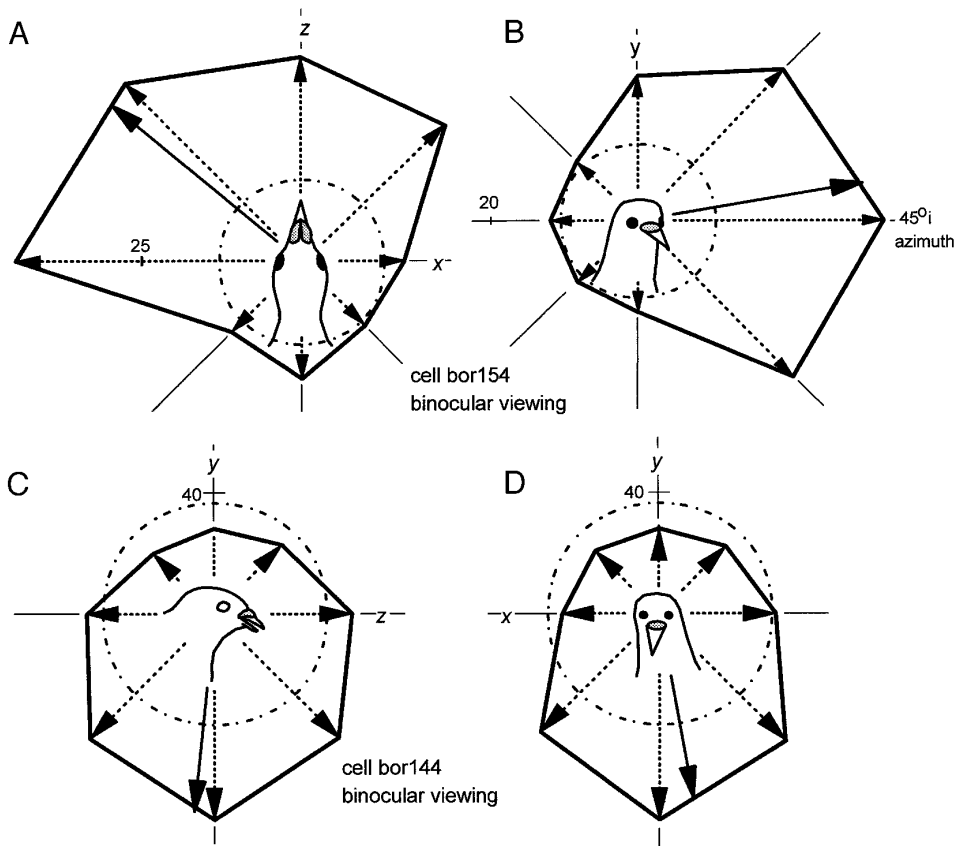


FIG. 2. Responses of $-x+z$ (A and B) and $-y$ (C and D) translation neurons. For the $-x+z$ neuron, a polar plot of azimuth tuning (in the horizontal plane) is shown in A, whereas elevation tuning in a vertical plane that intersects the horizontal plane at 45° ipsilateral (45°_i) azimuth is shown in B. This plane is illustrated in Fig. 1C. For the $-y$ neuron, C and D show elevation tuning in the sagittal and frontal planes, respectively. Broken circles represent the spontaneous firing rates, and the solid arrows, axes of maximal modulation from the best cosine fits.

the same direction of motion in the central areas of the both hemifields and were studied further with the translator. The other six neurons preferred the opposite direction of motion in the two hemifields and were studied further with the planetarium projector.

Neurons preferring translational optic flow along horizontal axes

Of the 31 neurons that preferred the same direction of motion in both hemifields, 28 preferred horizontal visual motion in both hemifields. Of these, 17 preferred temporal-to-nasal (T-N) motion, and 11 preferred nasal-to-temporal (N-T) motion in the central areas of both hemifields. Figure 1 shows the responses of a binocular neuron, (that preferred T-N motion in both eyes), to translational optic flow along numerous axes. A shows PSTHs in response to translation along eight directions in the horizontal plane (azimuthal tuning curve), whereas C shows PSTHs in response to translation in eight directions in the vertical plane orthogonal to the horizontal plane at 45° ipsilateral (45°_i) azimuth (i.e., the plane normal to the vector $+x+z$). The same data in A and B are shown in C and D, respectively, where the average firing rate is plotted as a function of the direction of translational optic flow, in polar coordinates (polar plots). In these and subsequent figures, the orientation of an arrow reflects the orientation of the axis of the translator, and the arrowheads point in the direction in which the animal would be moving to produce such a flowfield. That is, the arrowheads point toward the focus of expansion (FOE) in the flowfield. The large arrows in B and D indicate the peaks of the best

cosine fits to the tuning curves. These data show that this neuron was modulated maximally in response to translation along the horizontal axis oriented at $\sim 45^\circ_i$ azimuth but showed little modulation in response to translation along orthogonal axes [i.e., an horizontal axis oriented at 45° contralateral (45°_c) azimuth (A and B) and the y axis (axis 2 in C and D)]. Translation in the direction producing a focus of contraction (FOC) at 45°_i azimuth resulted in maximal excitation whereas translation in the opposite direction resulted in maximal inhibition. In vector notation, the best axis for this neuron is approximately $+x-z$. Figure 2, A and B, shows a neuron that also responded maximally to translational optic flow along an axis at 45°_i azimuth but showed the opposite direction preference to that in Fig. 1. Polar plots of azimuth tuning in the horizontal plane (A) and elevation tuning in a vertical plane normal to the vector $x+z$ (B) are shown. This neuron was excited maximally by a flowfield with an FOE at $\sim 45^\circ_i$ azimuth but, unlike most neurons, translation in the opposite direction along this axis did not result in inhibition below the spontaneous firing rate.

The best axes of the 28 neurons responsive to translational optic flow along horizontal axes are shown in Fig. 5, A and B. In A, the axes are from azimuth tuning curves and are projected onto the horizontal plane. Most of the best vectors fall in the lower right and upper left quadrants. Note the obvious clustering 45° to the midline in the bottom right quadrant ($+x-z$ neurons; $n = 17$), whereas a clustering is not as obvious in the upper left quadrant ($-x+z$ neurons; $n = 8$). The mean of the distribution of $+x-z$ neurons was 139.4°_c azimuth (large dashed arrow on the right in A). Elevation tuning curves were obtained from 11 of the 17

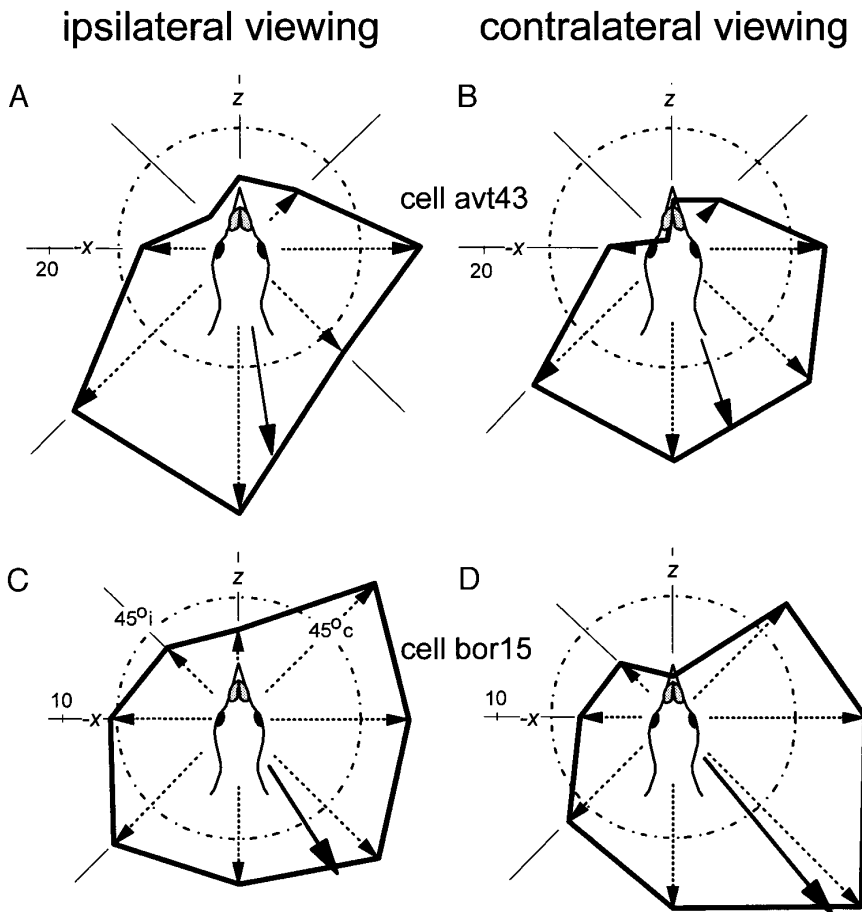


FIG. 3. Responses to translational optic flow in the horizontal plane under monocular viewing conditions is shown for 2 different neurons. *A* and *C*: polar plots of azimuth tuning under ipsilateral viewing conditions. *B* and *D*: contralateral viewing conditions. Broken circles, spontaneous firing rates; solid arrows, axes of maximal modulation from the best cosine fits. For the cell in *A* and *B*, the depth of modulation for ipsilateral and contralateral stimulation was approximately the same, whereas the cell in *C* and *D* showed a greater depth of modulation under contralateral viewing conditions. For both of these cells, the best response axis was similar under ipsilateral, contralateral and binocular viewing conditions.

$+x-z$ neurons. The elevation tuning was in the vertical plane intersecting the horizontal plane at 45°_i azimuth (illustrated in Fig. 1C) and the best axes from these tuning curves are shown on the left side in Fig. 5B. These vectors clustered near the horizontal plane (mean = -12.9° elevation). On the right side in *B*, the best axes of the eight $-x+z$ neurons from elevation tuning curves are shown. For simplicity, the best axes are shown as projected onto the vertical plane intersecting the horizontal plane at 45°_i azimuth, but in fact the elevation tuning was in this plane for only five of these neurons. Based on the best axes obtained from the azimuth tuning curves, the other three cells' elevation tuning was done in the sagittal plane. Nonetheless, note the clustering near the horizontal plane (mean = $+12.8^\circ$ elevation).

Neurons preferring translational optic flow along vertical axes

Three neurons responded best to upward motion in both eyes. Figure 2, *C* and *D*, shows the responses of one such neuron. Elevation tuning curves are shown in both the sagittal (yz) plane (*C*) and frontal (xy) plane (*D*). The cell was maximally excited by $-y$ translation (i.e., with the FOE below) and inhibited by $+y$ translation but was not modulated by optic flow along the z (*C*) or x (*D*) axes. Figure 5E shows the best axes of the three $-y$ neurons as projected onto the sagittal plane.

Responses to monocular stimulation

Responses to monocular stimulation of both the ipsilateral and contralateral hemifields was obtained for all 31 translation-sensitive neurons. Using criteria we have described elsewhere (Wylie et al. 1993), 23 cells were classified as having a marked contralateral ocular dominance (OD), 4 cells showed a slight contralateral OD, 1 cell showed a marked ipsilateral OD, and 1 cell was classified as equidominant, as the depth of modulation was approximately the same for stimulation of both hemifields. Two cells were classified as binocular obligate cells, as stimulation of the ipsi- and contralateral hemifields elicited no response or a very weak response, but they showed clear tuning when both eyes were stimulated simultaneously. For most cells (59%), binocular stimulation resulted in a greater depth of modulation than stimulation of the dominant eye alone. Across all cells, in response to translational optic flow along the preferred axes, the average ratio of the depth of modulation for binocular stimulation versus stimulation of the dominant eye alone was 1.23 ± 0.04 (mean \pm SE).

Figure 3, *A* and *B*, shows monocular azimuth tuning curves for the equidominant cell. With binocular stimulation, this cell preferred a translational optic flowfield along an horizontal axis oriented at $\sim 165^\circ_c$ azimuth. As indicated by the large arrows, the best axes as determined from the best cosine fits was approximately the same irrespective of the eye stimulated. This was also the case for the cell illustrated

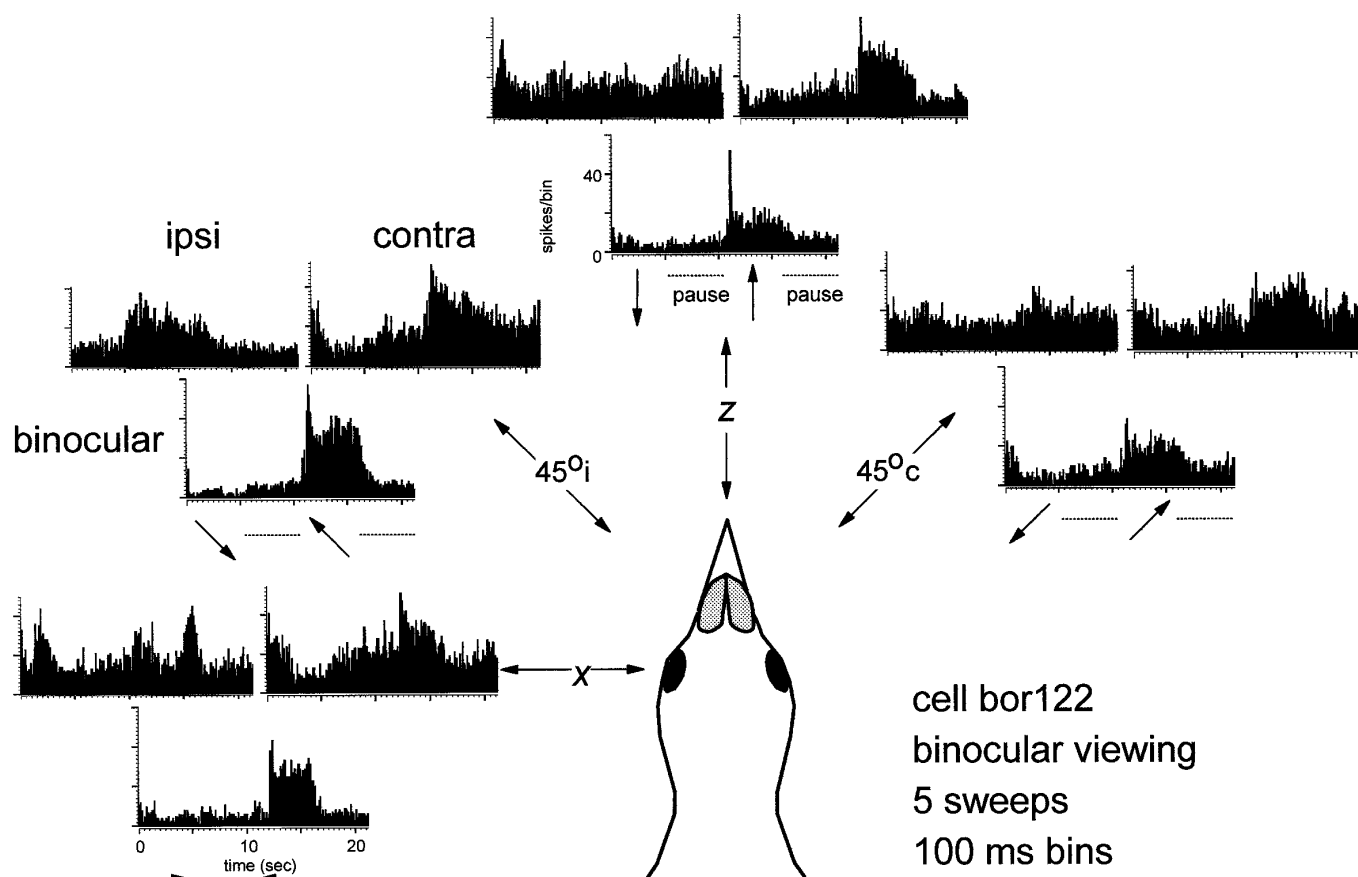


FIG. 4. Monocular and binocular responses of a $-x+z$ translation neuron to translational optic flow along axes in the horizontal plane. For each of the 4 axes, peristimulus time histograms (PSTHs) are shown for ipsilateral (*top left*), contralateral (*top right*), and binocular (*bottom*) viewing conditions. This cell showed similar responses under binocular and contralateral viewing conditions, although the depth of modulation was clearly greater for binocular stimulation. Responses under ipsilateral viewing conditions were somewhat enigmatic. For ipsilateral stimulation, there was no clear preferred axis, and transient responses can be seen in the PSTHs.

in Fig. 3, *C* and *D*, which showed a slight contralateral dominance. Note, however, that the azimuth tuning curve for ipsilateral stimulation was somewhat “sloppy.” In fact the correlation coefficient (r^2) of the best cosine fit to the tuning curve was 0.73, whereas for the binocular tuning curves, r^2 was usually greater than 0.9. For the cells with a marked contralateral dominance, the responses to stimulation of the ipsilateral eye were quite weak, (often below criteria). Complete ipsilateral tuning curves were obtained for 18 cells with a marked contralateral dominance. In nine instances we did not consider the cosine fit to the tuning curve to be reliable ($r^2 < 0.5$). Moreover in some cases, the responses to stimulation of the ipsilateral eye could be only called unusual. Figure 4 shows azimuth tuning for a $-x+z$ neuron that showed a marked contralateral OD. For each axis, PSTHs are shown for ipsilateral (*top left*), contralateral (*top right*), and binocular (*bottom*) stimulation. The tuning obtained with stimulation of the contralateral eye was clear, but this was not the case in response to ipsilateral stimulation. Numerous transients can be seen in these PSTHs, and they occurred in every sweep. Thus although the neuron responded to stimulation of the ipsilateral eye, there was no clear axis tuning as there was for stimulation of the contralateral eye. However, clearly the depth of modu-

lation was greater for binocular stimulation compared with stimulation of the dominant eye.

Figure 5, *C* and *D*, shows the best axes of $+x-z$ neurons from monocular azimuth tuning curves. Complete ipsi- and contralateral azimuth tuning curves were obtained from 14 cells and their best axes from contralateral stimulation are shown in *D*. *C* shows the best axes from ipsilateral stimulation, but only eight vectors are included. For the other six tuning curves, r^2 of the best cosine fit was < 0.5 . Comparing the data from *D* with that in *A*, it is apparent that the distribution of best axes in response to contralateral stimulation is similar to that in response to binocular stimulation, with an obvious clustering 45° to the midline. However, the vectors in response to ipsilateral stimulation (*C*) showed a much greater spread.

Cells responsive to rotational flowfields

In response to stimulation with the hand-held stimulus, six cells preferred opposite directions of motion in the two hemifields and were further studied with the *planetarium* projector. Three cells responded best to rotation about horizontal axes. Figure 6*B* shows an azimuth tuning curve in the horizontal plane for one such neuron. This neuron re-

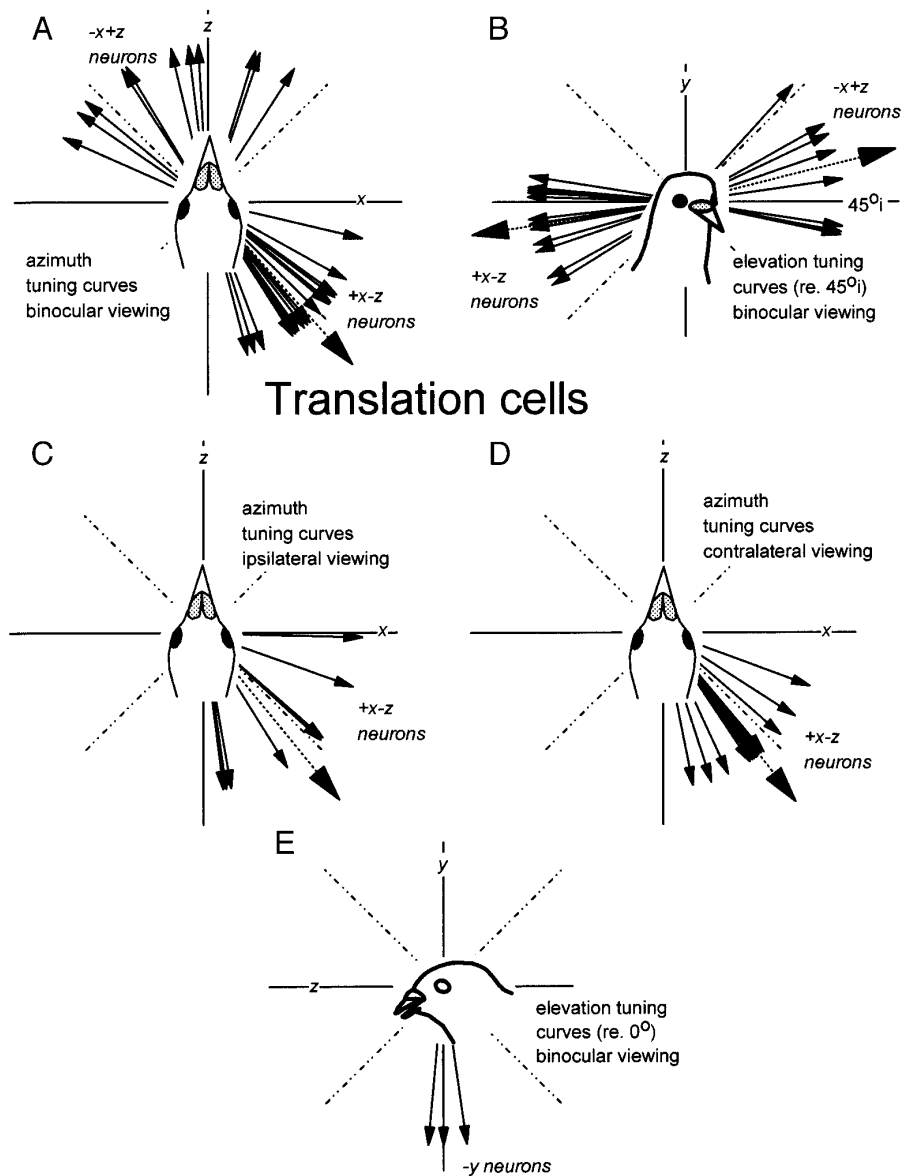


FIG. 5. Best axes of neurons responsive to translational optic flow. *A–D*: distribution of best axes for those neurons that preferred translational optic flow along axes in the horizontal plane. Longer arrows with broken shafts indicate the means of the respective distributions. *A*: best axes from azimuth tuning curves in the horizontal plane under binocular viewing conditions. Majority of these axes lie in the *top left* ($n = 8$) and *bottom right* ($n = 17$) quadrants. In the *bottom right quadrant*, there is an obvious clustering 45° to the midline ($+x-z$ translation neurons). In the *B, left*, we show the best axes of 11 of these $+x-z$ translation neurons determined from elevation tuning curves in the vertical plane that intersect the horizontal plane at 45° azimuth. (This plane is illustrated in Fig. 1C). *B, right*: best axes from elevation tuning curves for the 8 $-x+z$ translation neurons shown in *A, top left quadrant*. Axes are shown in the vertical plane that intersects the horizontal plane at 45° azimuth, but in fact the elevation tuning was in the sagittal plane for 3 of these neurons. *C and D*: best axes of neurons sensitive to translational optic flow along horizontal axes under ipsilateral and contralateral viewing conditions, respectively. *E*: best axes of neurons sensitive to translational optic flow along the vertical axis ($n = 3$).

sponded best to counterclockwise rotational optic flow about an horizontal axis oriented at $\sim 150^\circ$ azimuth (and clockwise rotational optic flow about an horizontal axis oriented at $\sim 30^\circ$ azimuth). The other two neurons preferred counterclockwise rotational optic flow about horizontal axes oriented at 37° and 155° azimuth.

Three cells responded best to rotation about the vertical axis. Figure 7, *A–C*, shows the responses of a neuron that was maximally excited by $+y$ rotation. In response to the hand-held stimulus, this cell preferred N-T motion in the contralateral eye and T-N motion in the ipsilateral eye. In *A*, PSTHs in response to rotation about four axes in the sagittal (yz) plane are shown. A polar plot of this elevation tuning in shown in *B*, whereas a polar plot of elevation tuning in the frontal (xy) plane for the same neuron is shown in *C*. The curved arrows indicate the direction of supposed head rotation, which is opposite to the direction of the resultant rotational flowfield. As evident by the best axes from both tuning curves, this cell was excited maximally by $+y$

rotation and maximally inhibited by $-y$ rotation. Rotation about the x and z axes produced comparatively little modulation. Figure 7, *D and E*, shows monocular elevation tuning curves in the sagittal plane for a neuron that preferred $-y$ rotation (*D*, contralateral; *E*, ipsilateral). This cell showed a marked contralateral OD (as did all 6 rotation-sensitive cells), but the best axis was approximately the same for both hemifields (a 24° difference). In response to binocular stimulation, the best axis was -94° elevation, which is closer to the best axis for ipsilateral stimulation than that for contralateral stimulation. For the third cell that preferred rotation about the vertical axis, a $+y$ neuron, the best axis was $+94^\circ$ elevation.

Location of the binocular neurons

In some experiments, we made electrolytic marking lesions such that the locations of responsive neurons could be identified. The binocular neurons were sometimes found

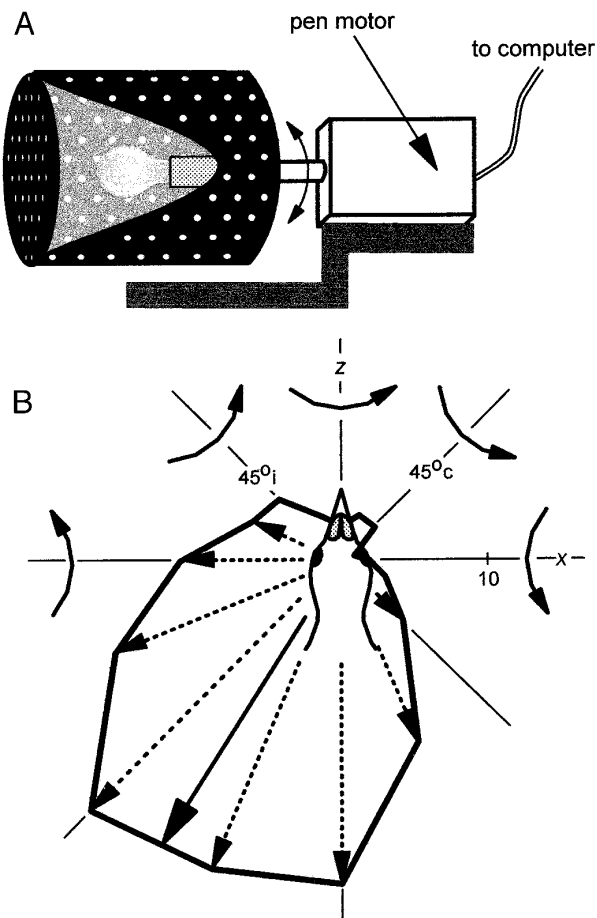


FIG. 6. Azimuth tuning curve in the horizontal plane for a $-x-z$ rotation neuron. *A*: planetarium projector used to produce rotational flowfields. It consisted of a hollow cylinder, the surface of which was pierced with numerous small holes. Part of the surface of the cylinder has been cut away to reveal the light source within, which cast a field of dots onto the walls, ceiling, and floor of the darkened room. A pen motor, driven by a waveform generator, oscillated the planetarium about its long axis. This effectively produced a rotational flowfield. *B*: polar plot of the responses of the neuron to rotational optic flow about 8 axes (22.5° apart) in the horizontal plane. Curved arrows, direction of head rotation that would produce the resultant flowfield. That is, the arrows are opposite to the direction of the optic flowfield. Solid arrow, axis of maximal modulation from the best cosine fit.

among the monocular units in nBOR proper (nBORp) (Brecha et al. 1980) but more commonly were found dorsal and caudal to the monocular units. Many of the binocular cells were localized in nBOR dorsalis (nBORd), a group of cells that surrounds nBORp dorsally and caudally (Brecha et al. 1980). In other cases, the binocular cells were found dorsal to the nBOR complex, in the mesencephalic reticular formation (MRF) and an area that appears to be a lateral extension of the Area Ventralis of Tsai (AVT). In Fig. 8 we show drawings of coronal sections through the nBOR illustrating the location of marking lesions (●) and the locations of monocular (m) and binocular (b) cells on those tracks. In *A*, a single electrode track is shown. A monocular cell was found in nBORp, but ~ 0.5 mm above the nBOR a binocular cell was isolated in the MRF. In *B*, three electrode penetrations in the same plane are shown through the caudal portion of nBOR. Binocular cells were found on the lateral

track in nBORd and on the medial track dorsal to nBORd in the lateral extension of AVT. Monocular cells were found on the central track in nBORp.

DISCUSSION

In this study we have shown that binocular neurons in nBOR of pigeons respond best to flowfields resulting from either self-translation or -rotation. These binocular neurons represent a small subpopulation of nBOR neurons, as most have monocular receptive fields in the contralateral eye (Burns and Wallman 1981; Morgan and Frost 1981; Wylie and Frost 1990a). It is difficult to estimate the percentage of binocular neurons as we did not sample the nucleus in any random procedure. Rather we actively searched for binocular cells. In fact, some of the neurons were localized outside of the boundaries of the nBOR in the MRF and AVT. Many others were found localized in nBORd, whereas the monocular cells were found within nBORp. This is consistent with anatomic studies that show there is a large projection from the contralateral nBOR to nBORd (Brecha et al. 1980). Collaterals of these fibers also appear to terminate outside the boundaries of nBOR in the adjacent AVT and MRF (Wylie et al. 1997). Thus the nBORd and adjacent AVT and RF appear to be a site of binocular integration of flowfield information. nBORd and the adjacent AVT are known to have different connections than nBORp. The projection to the inferior olive is largely from nBORd and much less from nBORp (Brecha et al. 1980). Likewise, the nBORd and AVT, but not nBORp, project heavily to areas of the dorsal thalamus where there is integration with the thalamofugal system and possibly the vestibular and somatosensory systems (Wylie et al. 1997, 1998b). Recently we have shown that information from nBORd reaches the hippocampus, both directly and via the AVT (Wylie and Glover 1998). nBORd also receives a massive input from the ipsilateral LM (Gamlin and Cohen 1988b) and the cerebellar nuclei (Arends and Ziegler 1991). Thus it seems that cells in the nBORd and adjacent AVT code higher-order flowfield information, either self-translation or -rotation. This information then is transferred along many pathways including an olivo-cerebellar pathway to the vestibulocerebellum (VbC), areas of the dorsal thalamus that project to numerous areas of the telencephalon, and to the hippocampus (Brecha et al. 1980; Wylie and Glover 1998; Wylie et al. 1997, 1998b).

Comparison with responses of VbC neurons

With the use of the translator and planetarium projectors, we could determine the axis preferences for translation and rotation-sensitive neurons, as we have done for complex spike activity of Purkinje cells in the VbC. In the flocculus of the VbC, cells prefer rotational optic flow about either the vertical axis or an horizontal axis oriented 45° to the midline (Wylie and Frost 1993). In the ventral uvula and nodulus, cells prefer translational optic flow along either a vertical axis or one of two horizontal axes oriented 45° to the midline (Wylie and Frost 1999; Wylie et al. 1998a). In the present study of the nBOR, we recorded from six cells that preferred rotational flowfields. Three of these cells preferred rotation about the vertical axis, and the other three

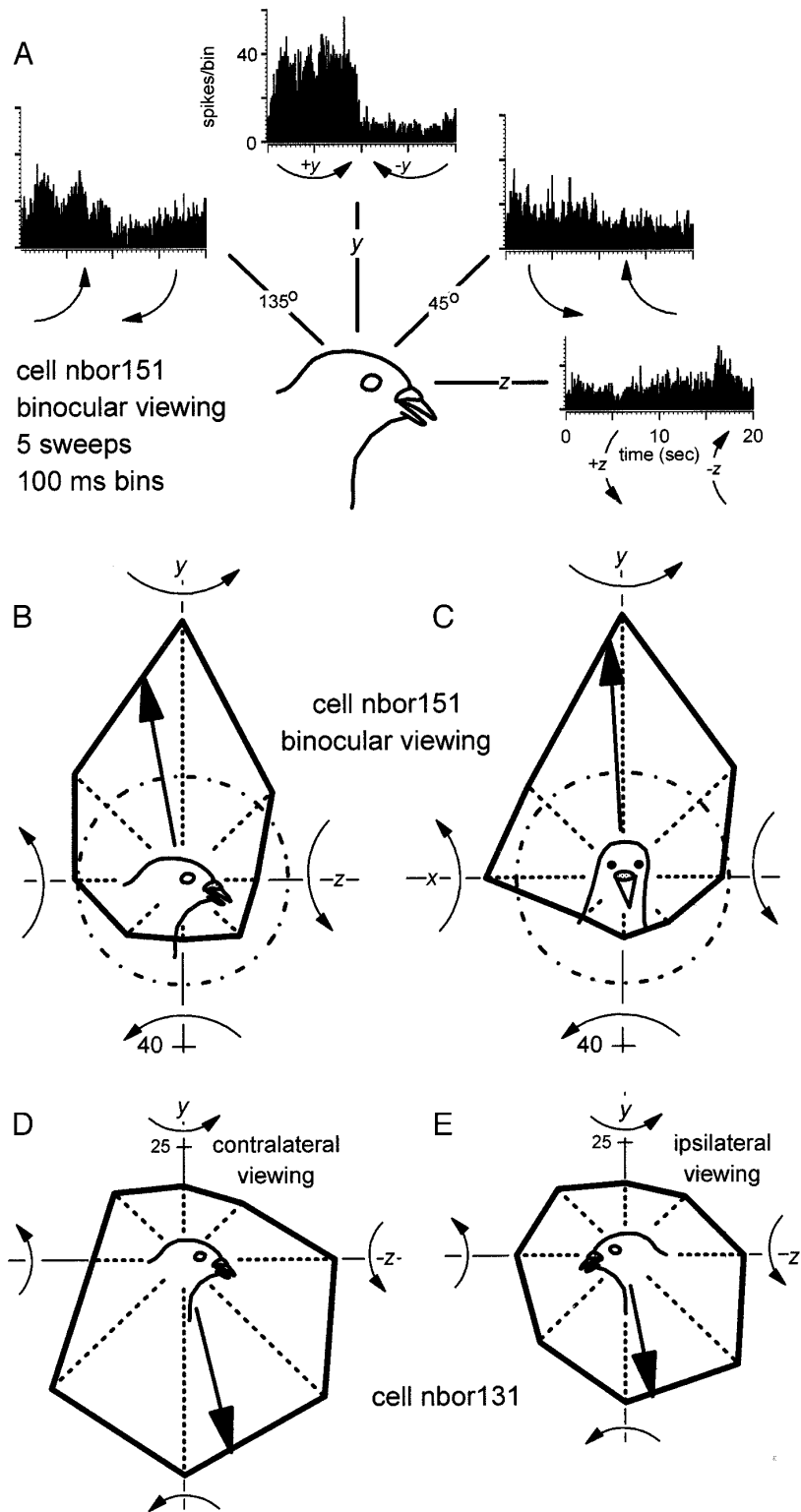


FIG. 7. Responses of neurons sensitive to rotation about the vertical axis. *A–C*: responses of a neuron that preferred $+y$ rotation. *A*: PSTHs in response to rotation about 4 axes in the sagittal plane. Each PSTH was summed from 5 sweeps, and each sweep consisted of 5 s of rotation about the axis in 1 direction, followed by 5 s of rotation in the opposite direction. Polar plot of these data are shown in *B*. *C*: polar plot of elevation tuning in the frontal plane is shown for the same neuron. *D* and *E*: responses of a $-y$ rotation neuron. Polar plots of elevation tuning in the sagittal plane is shown for contralateral (*D*) and ipsilateral (*E*) viewing. Broken circles, spontaneous firing rates; solid arrows, axes of maximal modulation from the best cosine fits. Arrows point in the direction of a head rotation which the animal would make to cause the flowfield, which is opposite to the direction of visual motion in the rotational flowfield. Note in *D* and *E* that the cell showed a contralateral ocular dominance and that the best axes for contralateral and ipsilateral stimulation differed by $\sim 20^\circ$.

preferred horizontal axes. It appears that rotation-sensitive binocular nBOR neurons share a similar reference frame to the flocculus Purkinje cells, but there is insufficient data to draw such a strong conclusion.

We also recorded from 31 cells that preferred translational flowfields. Three of these preferred translation along the vertical axes, whereas the remaining 28 pre-

ferred horizontal axes. Shown in Fig. 5A, within the distribution of the best axes of these 28 cells, there was a clear clustering in one quadrant 45° to the midline, but other best axes were distributed throughout the horizontal plane. Thus the three axes reference frame that is apparent in the complex spike (CS) activity of translation and rotation Purkinje cells (see companion paper) is not fully estab-

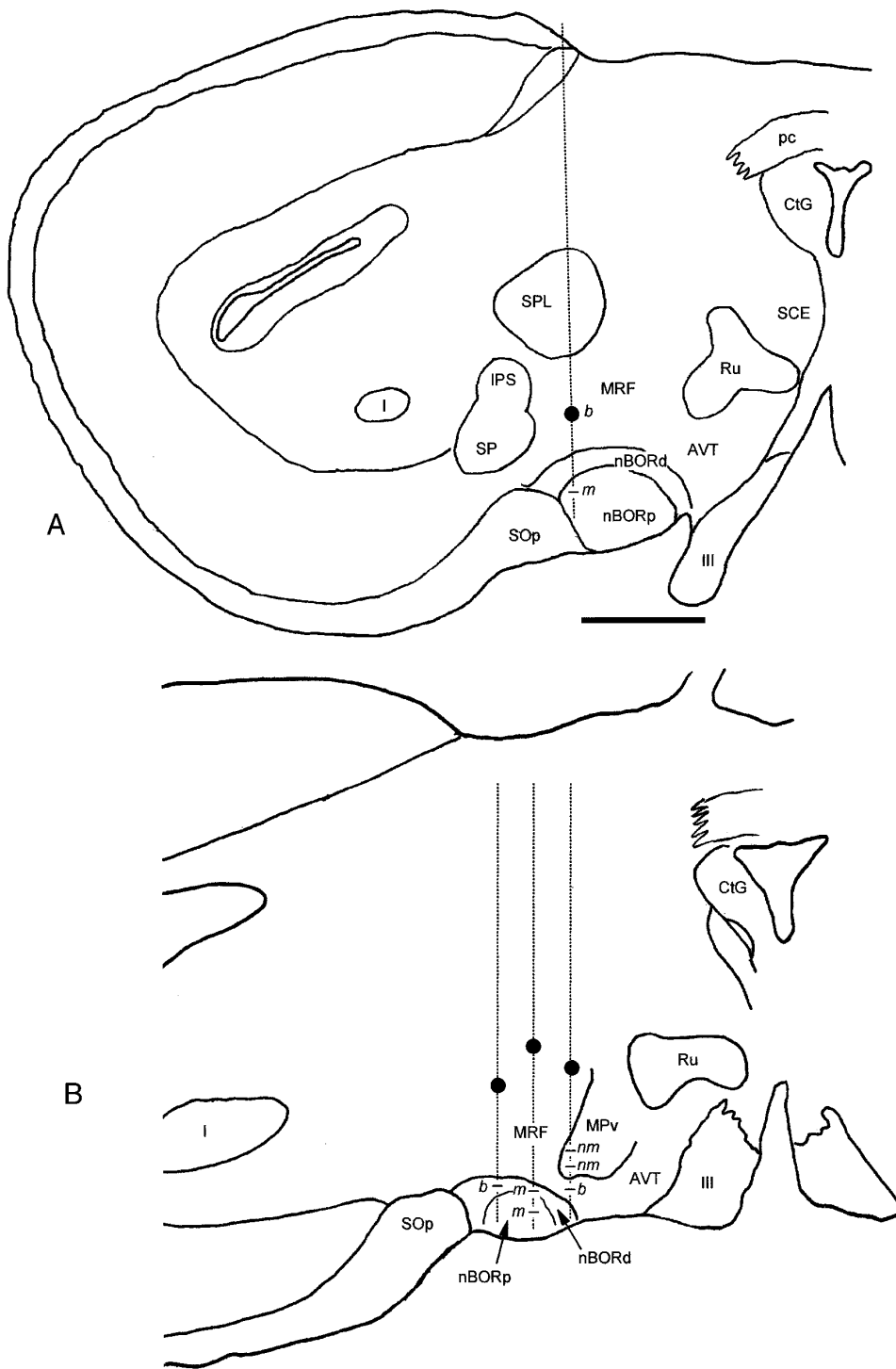


FIG. 8. Locations of binocular neurons in the vicinity of the nucleus of the basal optic root (nBOR). Data from 2 experiments are shown. ●, locations of electrolytic lesions. Locations of monocular (m), binocular (b), and nonmodulated (nm) neurons are shown. III, third cranial nerve; AVT, area ventralis of Tsai; CtG, central gray; I, nucleus isthmi; IPS, nucleus interstitio-preecto-subpretectalis; MRF, mesencephalic reticular formation; nBORd, nBOR pars dorsalis; nBORp, nBOR proper; pc, posterior commissure; Ru, nucleus ruber; SCE, stratum cellulare externum; SOp, stratum opticum; SPL, nucleus spiriformis lateralis; SP, nucleus subpretectalis.

lished in the nBOR. The nBOR (particularly nBORd), projects bilaterally to the medial column of the inferior olive (IO) (Brecha et al. 1980; Wylie et al. 1997), which in turn projects to the contralateral VbC as climbing fibers (CFs) (Arends and Voogd 1989; Lau et al. 1998). The LM also projects to the medial column (Clarke 1977; Gamlin and Cohen 1988b). Further integration of information of optic flow information from the nBOR and LM likely takes place in the IO to establish the three axis reference frame of the rotation and translation neurons

that is evident in the VbC. The fact that binocular nBOR neurons described in the present study generally exhibit a pronounced contralateral ocular dominance, whereas VbC cells exhibit a slight dominance or are equidominant (Wylie and Frost 1993, 1999; Wylie et al. 1993), is also suggestive that further integration takes place in the IO.

Finally, we must note that although we recorded from more translation- than rotation-sensitive cells, perhaps we have a sampling bias. As shown in the companion paper (Wylie and Frost 1999), cells responsive to translational

and rotational flowfields are equally abundant in VbC. We must emphasize that the binocular nBOR neurons represent a small subpopulation of cells. Thus when we did isolate binocular cells, subsequent penetrations were made in close proximity. Moreover, in subsequent animals, we usually made our initial penetrations in areas where we had isolated binocular neurons. As a result, the more rostral areas of the nBOR complex were not extensively explored.

This research was supported by grants from National Sciences and Engineering Research Council (to D.R.W. Wylie and B. J. Frost) and Alberta Heritage Foundation for Medical Research (to D.R.W. Wylie).

Address reprint requests to Douglas R. Wong-Wylie.

Received 15 January 1998; accepted in final form 28 September 1998.

REFERENCES

- ARENDS, J.J.A. AND VOGD, J. Topographic aspects of the olivocerebellar system in the pigeon. *Exp. Brain Res.* 17 Suppl.: 52–57, 1989.
- ARENDS, J.J.A. AND ZIEGLER, H. P. Organization of the Cerebellum in the Pigeon (*Columba livia*). II. Projections of the cerebellar nuclei. *J. Comp. Neurol.* 306: 245–272, 1991.
- BRECHA, N., KARTEN, H. J., AND HUNT, S. P. Projections of the nucleus of basal optic root in the pigeon: an autoradiographic and horseradish peroxidase study. *J. Comp. Neurol.* 189: 615–670, 1980.
- BURNS, S. AND WALLMAN, J. Relation of single unit properties to the oculomotor function of the nucleus of the basal optic root (AOS) in chickens. *Exp. Brain Res.* 42: 171–180, 1981.
- CLARKE, P.G.H. Some visual and other connections to the cerebellum of the pigeon. *J. Comp. Neurol.* 174: 535–552, 1977.
- FITE, K. V., BRECHA, N., KARTEN, H. J., AND HUNT, S. P. Displaced ganglion cells and the accessory optic system of the pigeon. *J. Comp. Neurol.* 195: 279–288, 1981.
- FROST, B. J., WYLIE, D. R., AND WANG, Y.-C. The analysis of motion in the visual systems of birds. In: *Perception and Motor Control in Birds*, edited by P. Green and M. Davies. Berlin: Springer-Verlag, 1994, p. 249–266.
- GAMLIN, P.D.R. AND COHEN, D. H. The retinal projections to the pretectum in the pigeon (*Columba livia*). *J. Comp. Neurol.* 269: 1–17, 1988a.
- GAMLIN, P.D.R. AND COHEN, D. H. Projections of the retinorecipient pretectal nuclei in the pigeon (*Columba livia*). *J. Comp. Neurol.* 269: 18–46, 1988b.
- GIBSON, J. J. The visual perception of objective motion and subjective movement. *Psychol. Rev.* 61: 304–314, 1954.
- GIOANNI, H., REY, J., VILLALOBOS, J., AND DALBERA, A. Single unit activity in the nucleus of the basal optic root (nBOR) during optokinetic, vestibular and visuo-vestibular stimulations in the alert pigeon (*Columba livia*). *Exp. Brain Res.* 57: 49–60, 1984.
- GRASSE, K. L. AND CYNADER, M. S. The accessory optic system in frontal-eyed animals. In: *Vision and Visual Dysfunction. The Neuronal Basis of Visual Function*, edited by A. Leventhal. New York: MacMillan, 1990, vol. IV, p. 111–139.
- KARTEN, H. J. AND HODOS, W. *A Stereotaxic Atlas of the Brain of the Pigeon (Columba livia)*. Baltimore: Johns Hopkins Press, 1967.
- KARTEN, H. J., FITE, K. V., AND BRECHA, N. Specific projection of displaced retinal ganglion cells upon the accessory optic system in the pigeon (*Columba livia*). *Proc. Natl. Acad. Sci. USA* 74: 1752–1756, 1977.
- LAU, K. L., GLOVER, R. G., LINKENHOKER, B., AND WYLIE, D.R.W. Topographical organization of inferior olive cells projecting to translation and rotation zones in the vestibulocerebellum of pigeons. *Neuroscience* 85: 605–614, 1998.
- McKENNA, O. AND WALLMAN, J. Identification of avian brain regions responsive to retinal slip using 2-deoxyglucose. *Brain Res.* 210: 455–460, 1981.
- McKENNA, O. AND WALLMAN, J. Functional postnatal changes in avian brain regions responsive to retinal slip: a 2-deoxy-D-glucose study. *J. Neurosci.* 5: 330–342, 1985.
- MORGAN, B. AND FROST, B. J. Visual response properties of neurons in the nucleus of the basal optic root of pigeons. *Exp. Brain Res.* 42: 184–188, 1981.
- REINER, A., BRECHA, N., AND KARTEN, H. J. A specific projection of retinal displaced ganglion cells to the nucleus of the basal optic root in the chicken. *Neuroscience* 4: 1679–1688, 1979.
- SIMPSON, J. I. The accessory optic system. *Annu. Rev. Neurosci.* 7: 13–41, 1984.
- SIMPSON, J. I., GIOLLI, R. A., AND BLANKS, R.H.I. The pretectal nuclear complex and the accessory optic system. In: *Neuroanatomy of the Oculomotor System*, edited by J. A. Buttner-Ennever. Amsterdam: Elsevier, 1988a, p. 335–364.
- SIMPSON, J. I., GRAF, W., AND LEONARD, C. The coordinate system of visual climbing fibres to the flocculus. In: *Progress in Oculomotor Research*, edited by A. F. Fuchs and W. Becker. Amsterdam: Elsevier, 1981, p. 475–484.
- SIMPSON, J. I., LEONARD, C. S., AND SOODAK, R. E. The accessory optic system of rabbit. II. Spatial organization of direction selectivity. *J. Neurophysiol.* 60: 2055–2072, 1988b.
- WINTERSON, B. J. AND BRAUTH, S. E. Direction-selective single units in the nucleus lentiformis mesencephali of the pigeon (*Columba livia*). *Exp. Brain Res.* 60: 215–226, 1985.
- WOLF-OBERHOLLENZER, F. AND KIRSCHFELD, K. Motion sensitivity in the nucleus of the basal optic root of the pigeon. *J. Neurophysiol.* 71: 1559–1573, 1994.
- WYLIE, D.R.W., BISCHOF, W. F., AND FROST, B. J. Common reference frame for the coding translational and rotational optic flow. *Nature* 392: 278–282, 1998a.
- WYLIE, D. R. AND FROST, B. J. Binocular neurons in the nucleus of the basal optic root (nBOR) of the pigeon are selective for either translational or rotational visual flow. *Vis. Neurosci.* 5: 489–495, 1990b.
- WYLIE, D. R. AND FROST, B. J. Visual response properties of neurons in the nucleus of the basal optic root of the pigeon: a quantitative analysis. *Exp. Brain Res.* 82: 327–336, 1990a.
- WYLIE, D. R. AND FROST, B. J. Responses of pigeon vestibulocerebellar neurons to optokinetic stimulation. II. The 3-dimensional reference frame of rotation neurons in the flocculus. *J. Neurophysiol.* 70: 2647–2659, 1993.
- WYLIE, D.R.W. AND FROST, B. J. The pigeon optokinetic system: visual input in extraocular muscle coordinates. *Vis. Neurosci.* 13: 945–953, 1996.
- WYLIE, D.R.W. AND FROST, B. J. Complex spike activity of Purkinje cells in the ventral uvula and nodulus of pigeons in response to translational optic flowfields. *J. Neurophysiol.* 81: 256–266, 1999.
- WYLIE, D.R.W. AND GLOVER, R. G. The hippocampus receives optic flow information from the accessory optic system: support for the path integration hypothesis. *Soc. Neurosci. Abstr.* 24: 1909, 1998.
- WYLIE, D.R.W., GLOVER, R. G., AND LAU, K. L. Projections from the accessory optic system and pretectum to the dorsolateral thalamus in the pigeon (*Columba livia*): a study using both anterograde and retrograde tracers. *J. Comp. Neurol.* 391: 456–469, 1998b.
- WYLIE, D. R., KRIPALANI, T.-K., AND FROST, B. J. Responses of pigeon vestibulocerebellar neurons to optokinetic stimulation. I. Functional organization of neurons discriminating between translational and rotational visual flow. *J. Neurophysiol.* 70: 2632–2646, 1993.
- WYLIE, D.R.W., LINKENHOKER, B., AND LAU, K. L. Projections of the nucleus of the basal optic root in pigeons (*Columba livia*) revealed with biotinylated dextran amine. *J. Comp. Neurol.* 384: 517–536, 1997.